

# Review

## Factors affecting particle-coarsening kinetics and size distribution

C. S. JAYANTH, PHILIP NASH

*Department of Metallurgical and Materials Engineering, Illinois Institute of Technology, Chicago, Illinois 60616, USA*

The Lifshitz-Slyozov-Wagner (LSW) theory was developed to model kinetics of precipitate growth from supersaturated solid solutions. The theory corresponds to a zero volume fraction approximation but has been modified for finite volume fractions in order to correspond to real situations. The LSW theory has been applied to study coarsening of grains in liquid-phase sintering and to the coarsening of pores in solid-state sintering systems. There are some additional factors not considered in the LSW theory which can influence the coarsening kinetics depending on the system. It is important, therefore, to incorporate these factors into a coarsening model for better analysis of experimental data. The experimental evidence for the effects of these additional factors is reviewed together with the theoretical modifications made to the basic LSW theory in order to incorporate these factors.

### Nomenclature

$r$	Radius of the particle	$E_1$	Elastic strain energy due to lattice mismatch between precipitate and matrix
$r_c$	Critical particle radius	$E_3$	Elastic interaction energy due to overlapping of strain fields
$C_r$	Solute concentration in equilibrium with a particle of radius $r$	$\mu$	Shear modulus of the matrix
$C_e$	Solute concentration in equilibrium with a particle of infinite radius	$\mu'$	Shear modulus of the precipitate
$\sigma$	Particle/matrix interfacial energy	$\tau_g$	Time between contacts due to gravity
$\alpha, \gamma$	Constant	$\tau_{br}$	Time between contacts due to Brownian motion
$V_m$	Molar volume of the precipitate	$\tau_f$	Time required to fuse two particles
$\bar{r}$	Mean radius of the particle at time $t$	$\tau_{or}$	Time required to remove a particle by Ostwald ripening
$\bar{r}_0$	Mean radius of the particle at the onset of coarsening	$U_A$	Driving force correction factor
$Q$	Volume fraction of the precipitate	$X_B^{os}$	Solubility of component $B$ in the solid phase
$k_T^2$	Sink factor	$k_{LSW}$	LSW rate constant
$D_{eff}$	Effective diffusion coefficient	$J_{it}^s$	Flux of the $i$ th component for the $s$ th phase
$D_{gb}$	Diffusion coefficient along the grain boundary	$D_i$	Diffusion coefficient of the $i$ th component
$D_d$	Diffusion coefficient along the dislocation	$\bar{c}_i$	Average concentration of $i$ th component in the matrix
$Z$	Number of dislocation lines crossing the surface	$c_{it}^s$	Equilibrium concentration of the $i$ th component at the $s$ th phase particle/matrix interface
$q$	Dislocation pipe cross-section	$\varrho$	Equal to $r/\bar{r}$
$l$	Average length of the dislocation		

### 1. Introduction

Although the theoretical model of coarsening was developed almost 30 years ago [1-4] and successfully predicts coarsening kinetics qualitatively, we are still not able to apply it with confidence to the quantitative determination of parameters such as effective diffusion coefficient and interfacial energy. The major problem has been that the theory is clearly deficient in not taking into account several important factors affecting coarsening kinetics. A number of modifications of the basic theory have been proposed but none of these has found general acceptance and none account for all of the factors which can affect coarsening.

The problem of the growth of precipitates by diffusion of solute in a matrix was first treated by Greenwood [1]. The basic equations which form the beginning of the analysis are the Gibbs-Thomson equation for the concentration of solute in equilibrium with a particle of radius,  $r$

$$C_r = C_e \exp(2\sigma V_m / RT r) \quad (1)$$

and Fick's law for the diffusion flux,  $j$

$$j = -D \left( \frac{\partial C}{\partial r} \right) \quad (2)$$

where  $C_r$  is the concentration of the solute at the

particle/matrix interface in equilibrium with a particle of radius  $r$ ,  $C_c$  is the solute concentration in equilibrium with a particle of infinite size,  $\sigma$  is the particle/matrix surface energy,  $V_m$  is the molar volume of solute,  $D$  is the diffusivity and  $RT$  has its usual meaning.

The theory of coarsening was further developed by Lifshitz and Slyozov [2, 3] and independently by Wagner [4], commonly known as the LSW theory, to model the kinetics of precipitate growth from supersaturated solid solutions after the completion of nucleation. The LSW theory corresponds to a zero volume fraction approximation which obviously does not correspond to real situations. Because of this, considerable effort has gone into modifying the basic theory to allow for finite volume fractions of precipitate and also to allow for other factors affecting the coarsening kinetics.

The theory of particle coarsening involves solution of three basic equations. These are: (i) the kinetic equation which gives the growth rate of an individual particle and is derived from the flux equation and the Gibbs–Thomson equation; (ii) equation of continuity which must be obeyed by the particle-size distribution; and (iii) a conservation equation for which the solution of (i) must be acceptable.

The kinetic equation for the dimensionless growth rate,  $g$ , using the notation of Lifshitz and Slyozov, is given by

$$-g = \frac{dz}{d\tau} = (z^{1/3} - 1)\gamma - z \quad (3)$$

where  $z$  is a dimensionless parameter given by the ratio of the particle volume to the volume of a particle of critical size, i.e.  $z = r^3/r_c^3$  where  $r_c$  and  $r$  are the critical and actual particle radius at time  $t$ , respectively.  $\tau$  is a dimensionless parameter of time given by  $\ln(r_c^3/r_0^3)$  and  $r_0$  is the critical particle radius at the onset of coarsening. The quantity  $\gamma$  is given by

$$\gamma = \frac{dt'}{dx^3} \quad (4)$$

where  $x = r_c/r_0$  and  $t'$  is a dimensionless quantity proportional to the real time  $t$  and is given by

$$t' = \frac{2\sigma V_m CDt}{r_0^3 RT} \quad (5)$$

The rate equation in the LSW theory derived from Equations 3, 4 and 5 is

$$\bar{r}^3 - \bar{r}_0^3 = kt \quad (6)$$

and

$$k = \frac{8\sigma V_m^2 DC_c}{9RT} \quad (7)$$

where  $\bar{r}$  is the mean radius of the particles at time  $t$ ,  $\bar{r}_0$  is the mean radius of the particles at time  $t = 0$ , i.e. at the start of coarsening,  $k$  is the rate constant and  $R$  is the gas constant. The continuity equation is given by

$$\frac{d}{dz}(\phi'g) + \phi' = 0 \quad (8)$$

where  $g = -(dz/d\tau)$  from Equation 1 and  $\phi'$  is a function of  $z$  only.

The conservation equation imposes a condition to the effect that the quantity of matter in a defined system remains constant. For a long ageing time it reduces to

$$K \int_0^\infty \phi'z dz = 1 \quad (9)$$

where  $K = 4\pi r_{c0}^3/3Q$  with  $Q$  = volume fraction of precipitate.

Although the LSW theory was developed to study the kinetics of precipitate growth from supersaturated solid solution, it has also been applied to coarsening of grains in liquid-phase sintering [5–8] and to the coarsening of pores in solid-state sintering [9, 10]. There are, however, some additional factors not considered in the LSW theory which might influence the kinetics of coarsening to different degrees depending on the system under study. Some comparisons between theory and experiment in the literature may have led to incorrect conclusions because important factors affecting the coarsening kinetics were ignored. We will now look at these factors and consider the experimental evidence for each of them and their effect on the coarsening kinetics.

The factors considered to affect coarsening are:

- (1) volume fraction of second phase;
- (2) short-circuit diffusion paths such as surfaces, grain boundaries and dislocations;
- (3) elastic strain due to precipitate/matrix mismatch;
- (4) elastic interactions between precipitates;
- (5) loss of coherency;
- (6) diffusion, interface or intermediate type of growth control;
- (7) particle motion;
- (8) thermodynamically non-ideal systems;
- (9) multi-phase precipitates;
- (10) external stresses;
- (11) irradiation.

Among the factors listed above, 10 and 11 will not be discussed here because these are externally imposed factors which can be removed. All systems will be influenced by one or more of the above factors.

The LSW theory successfully predicts  $(\text{size})^3 \propto t$  and the total number of particles per unit volume,  $N_v \propto t^{-1}$ , but it gives a poor prediction of size distribution. This is evident from Fig. 1 which compares the LSW distribution with that determined experimentally [11] from an Ni–22 at % Co–13 at % Al alloy. From experimental comparisons of rate constant it is difficult to assess whether the theory predicts good values or not because of a lack of knowledge of the parameters involved. It is important, therefore, to incorporate the above mentioned factors into a coarsening model for better analysis of experimental data and increase confidence in the parameter values thus derived. It should be recognized that Lifshitz and Slyozov [2, 3] have outlined some of the necessary modifications to the original theory for several factors, namely, elastic stresses and encounters.

## 2. Volume fraction effect

As mentioned earlier, the LSW theory is applicable only when the volume fraction of the precipitate is

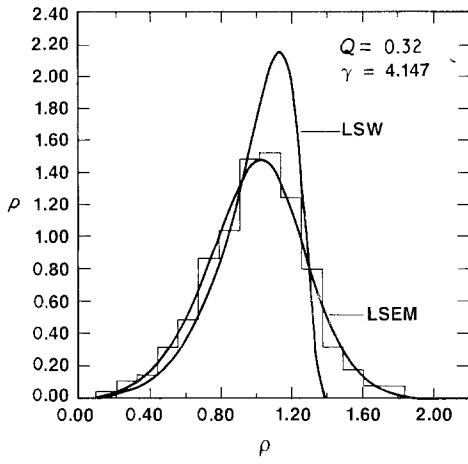


Figure 1 Comparison of the LSW and LSEM distribution function with an experimental distribution for Ni<sub>3</sub>Al-type precipitates in an alloy of nickel plus 22 at % Co and 13 at % Al. The volume fraction of precipitate in the alloy is 0.32 [11].

essentially zero. The LSW theory predicts the average particle volume to increase linearly with time and also predicts an asymptotic particle size distribution resulting from coarsening. Experimental measurements in systems where the volume fraction is greater than zero show that  $\bar{r}^3 \propto t$  and  $N_v \propto t^{-1}$  but the particle-size distributions are broader than predicted by the theory. In the LSW theory, Zener's approximation was adopted for the diffusion geometry, i.e. the growth rate is given by

$$\frac{dr}{dt} = \frac{D(C - C_r)}{r} \quad (10)$$

Here  $C$  is the concentration of solute in the matrix in equilibrium with a particle of infinite radius. Equation 10 becomes a poor approximation as the inter-particle distance decreases, corresponding to an increasing volume fraction, because the diffusion fields begin to overlap. In many commercial alloys second-phase volume fractions of  $\approx 60\%$  are encountered, therefore, the volume fraction effect is of considerable importance.

Ardell [12] proposed a modification of the LSW theory, modifying the diffusion equation to take into account the volume fraction by using a more realistic diffusion geometry. In that theory the rate constant,  $k$ , is very sensitive to volume fraction. Tsumuraya and Miyata [13] have used several alternative diffusion geometries to predict theoretically the particle-size distributions (PSD). They used the full width at half maximum (FWHM) to compare the theoretical and experimental PSDs. These PSDs change in skewness as the volume fraction increases [11, 14]. For such distributions FWHM is a crude measure of the PSD and comparison with theoretical PSDs is better performed using statistical parameters such as coefficient of skewness, coefficient of kurtosis and standard deviation [15]. Asimov [16] also modified the coarsening theory by modifying the diffusion geometry. These modifications [12, 13, 16] fail to perform the statistical averaging of the diffusional interactions between particles that is necessary for a satisfactory solution to this problem.

Brailsford and Wynblatt (BW) [17] overcame this problem by using chemical rate theory to perform the statistical averaging. Glicksman and Voorhees [18, 19] approached the problem of multi-particle diffusion using computer simulation techniques. Marqusee and Ross [20] used a statistical method and Tokuyama and Kawasaki [21] proposed a statistical mechanical theory approach to model coarsening. The differences between these theories have been discussed in detail by Voorhees [22] and will not be reiterated here. All of these theories [17–21] account for the volume fraction of second-phase particles and also have an identical basic approach, but the final results are quantitatively different. Because the chemical rate theory approach of BW has been further developed and applied to experimental coarsening data, a brief discussion of the BW theory follows. The growth rate equation according to BW is

$$v(r, t) = \frac{DW(r, R_1)}{r} \left( \frac{\int_0^\infty rW(r, R_1)f(r, t)\bar{c} dr}{\int_0^\infty rW(r, R_1)f(r, t) dr} - \bar{c}(r) \right) \quad (11)$$

where

$$W(r, R_1) = \frac{1 + k_T R_1}{1 + k_T(R_1 - 1)} \quad (12)$$

Here  $k_T$  is the square root of the sink factor and  $R_1 = rQ^{-1/3}$ . In their subsequent development of the theory,  $R_1$  was approximated by  $r$  which results in an expression for  $W(r, R_1) = (1 + k_T R_1)$ . The final rate equation due to BW [17] is

$$\bar{r}^3 - \bar{r}_0^3 = kt \quad (13)$$

and

$$k = \frac{6\sigma V_m DC_c}{k_B T \alpha} \left( \frac{\bar{r}}{r_c} \right) \quad (14)$$

where

$$\alpha = \frac{2\sigma V_m DC_c}{k_B T r_c^2} \left( \frac{dt}{dr_c} \right) \quad (15)$$

The self-consistent development of the BW theory using Equation 12 has been made by Stevens [14] and the resulting theory is referred to as the Brailsford Wynblatt self consistent theory (BWSC).

None of these theories takes into account the observed phenomenon of particle coalescence. Coalescence is a volume-fraction effect in addition to the overlap of diffusion fields. The effect of coalescence or encounters between particles has been investigated by Davies *et al.* [11, 23] based on the theoretical treatment outlined by Lifshitz and Slyozov [2] and this modification is termed the Lifshitz–Slyozov encounter modified (LSEM) theory. It is assumed that coalescence occurs instantaneously when two particles encounter, i.e. two particles are removed from the smaller size ranges in the distribution and one is added to the larger size ranges. This effect adds a term to the continuity Equation 8

$$\frac{d}{dz}(\phi g) + \phi = \frac{-3Q}{4\pi} I \quad (16)$$

where  $\phi = K\phi'$ .  $I$  is the encounter integral and is

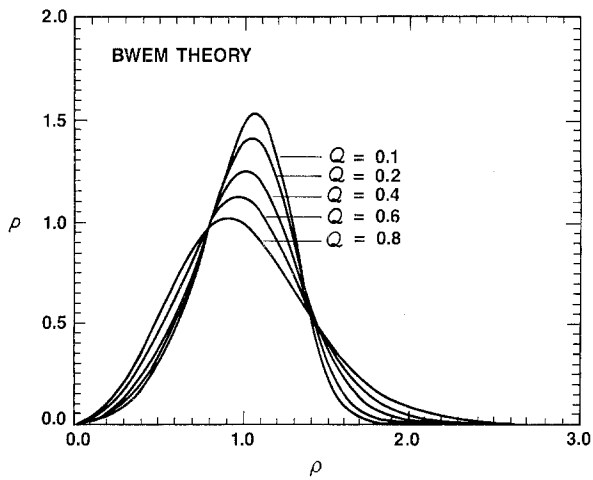


Figure 2 BWEM particle-size distribution as a function of volume fraction of the precipitate,  $Q$ .

given by

$$I = \frac{1}{2} \int_0^z z \phi(z - z') \phi(z') dz' - \phi(z) \int_0^\infty (z + z') \phi(z') dz' \quad (17)$$

This development leads to broader PSDs than the LSW theory, as do other theoretical modifications. The predicted LSEM particle-size distribution for a volume fraction of 0.32 may be compared in Fig. 1 with the LSW distribution and an experimental distribution. Coalescence should be important in liquid-matrix systems but may be reduced in solid-state systems because of matrix strains around precipitates. In solid-state systems, particles may have ordered structures and coalescence might lead to the formation of APBs, which generally have much larger interfacial energies than particle/matrix interfaces. In this case there will be a resistance to coalescence and the effect of this mechanism on coarsening will be reduced. Recently, the BWSC [14, 21] theory has been incorporated [14] into the LSEM theory and this modification is designated the Brailsford Wynblatt encounter modified (BWEM) theory. The sensitivity of  $k$  with the volume fraction is greater than that predicted by the LSEM theory. The PSDs for finite volume fractions are broader than the LSW distributions, Fig. 2, comparing more favourably with experiment.

Fig. 3 shows the variation of the ratio of the theoretically predicted rate constant, for the theories described above, to the LSW rate constant, as a function of volume fraction. To test the validity of various theories it is not practical to compare the theoretical and the experimental PSDs as the number of particles needed for statistically significant data is very large. Although large quantities of data may be gathered automatically using image analysis systems, these do not seem to have been used to obtain such data and this is probably due to difficulties in processing images containing particles which may be overlapping or which have poorly defined edges. Comparison of the measured variation of  $k$  as a function of volume fraction with theoretical predictions provides a simpler method of testing different theories.

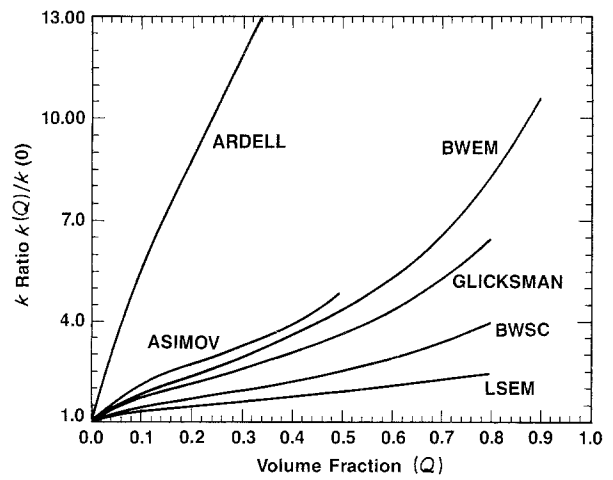


Figure 3 Variation of  $k$  ratio with volume fraction according to various theories.

Some experimental work [24–29] has been done specifically to study the effect of volume fraction on rate constant,  $k$ , in nickel base alloys. The absolute values of the predicted rate constants cannot easily be compared with experimental values because of a lack of information regarding  $\sigma$  and  $D$ . Most investigations [24–26, 28–31] fail to show a volume fraction effect. In multi-component systems the situation becomes more complex. This can be seen from the work of Biss and Sponseller [32] in their study on the effect of molybdenum on the coarsening of  $\gamma'$  in Ni–Al–Cr and Ni–Al–Cr–Ti alloys. From their results on Ni–Al–Cr alloys it has been observed [27] that the value of  $k$  at 42% volume fraction is greater than that at 9% volume fraction, which is contrary to the observation made by Chellman and Ardell [25]. The measured change in the rate constant is about 1.7. The LSEM and the BWEM theories predict a variation of 1.4 and 2.1, respectively. Both theories therefore provide good agreement. Work done by Sorokina and Yuganova [33] on Ni–Al–Cr–Ti alloys show a dependence of  $k$  on volume fraction although they failed to point this out [27]. Table I shows the rate constant determined for various systems by several workers. A point to be observed is that the alloys chosen for study by some workers [23, 26, 32] do not necessarily lie on the same tie line. This would bring in the effect of compositional variation of the phases in the alloys to the measured growth kinetics, making it difficult to draw conclusions about the effect of volume fraction.

The LSW theory has been applied to the analysis of the behaviour of liquid-phase sintering systems. Kang and Yoon [5, 6] have compared  $k$  in Co–Cu and Fe–Cu alloys to that predicted by various theories, namely Ardell's, LSEM and BW, and they noted that their experimental  $k$  values did not agree. The reasoning given by them [5] for the disagreement is that the shape of the coarsening particles was not spherical as assumed in all the theories. But comparing the experimental  $k$  values with the BWEM [14] theory, Table II gave much better agreement, indicating that taking into account the occurrence of encounter events and choosing the proper diffusion geometry can result in better agreement with experiment. From Table II it is

TABLE I Coarsening-rate constants,  $k$ , for various systems

Alloy	Temp. (K)	Volume fraction	$k$ ( $\text{m}^3 \text{sec}^{-1}$ )	Reference
Ni-6.35Al	898	0.145	$2.12 \times 10^{-30}$	[24]
Ni-6.71Al	898	0.198	$2.00 \times 10^{-30}$	
Ni-6.35Al	988	0.091	$7.25 \times 10^{-29}$	
Ni-6.71Al	988	0.148	$6.77 \times 10^{-29}$	
Ni-6.71Al	1023	0.125	$1.59 \times 10^{-28}$	
Ni-6.71Al	1048	0.102	$3.61 \times 10^{-28}$	
Ni-7Al	1073	0.090	$1.10 \times 10^{-27}$	[25]
Ni-8Al	1073	0.270	$1.06 \times 10^{-27}$	
Ni-9Al	1073	0.440	$1.20 \times 10^{-27}$	
Ni-9.9Al	1073	0.600	$1.30 \times 10^{-27}$	
Ni-16.9Cr-3.4Al	1023	0.275	$5.11 \times 10^{-29}$	
Ni-14.2Cr-4.9Al	1023	0.420	$5.11 \times 10^{-29}$	
Ni-40.0Co-17.2Cr-4Ti	1073	0.103	$1.76 \times 10^{-29}$	[26]
Ni-40.0Co-17.0Cr-5Ti	1073	0.140	$1.76 \times 10^{-29}$	
Ni-34.6Co-16.8Cr-6Ti	1073	0.196	$1.82 \times 10^{-29}$	
Ni-40.0Co-17.2Cr-4Ti	1173	0.075	$3.41 \times 10^{-28}$	
Ni-40.0Co-17.0Cr-5Ti	1173	0.100	$3.23 \times 10^{-28}$	
Ni-39.6Co-16.8Cr-6Ti	1173	0.167	$3.40 \times 10^{-28}$	
Ni-20Cr-3.5Al	1023	0.190	$8.13 \times 10^{-29}$	[29]
Ni-20Cr-4.2Al	1023	0.260	$8.13 \times 10^{-29}$	
Ni-20Cr-4.4Al	1023	0.340	$8.13 \times 10^{-29}$	
Ni-20Cr-6.2Al	1023	0.600	$8.13 \times 10^{-29}$	
Ni-20Cr-1.6Ti-0.85Al	1023	0.050	$5.63 \times 10^{-29}$	[31]
Ni-20Cr-2.6Ti-1.60Al	1023	0.190	$1.60 \times 10^{-29}$	
Ni-20Cr-3.0Ti-2.20Al	1023	0.310	$1.60 \times 10^{-29}$	
Ni-20Cr-4.9Nb-1.75Al	1023	0.140	$2.50 \times 10^{-29}$	
Ni-20Cr-6.3Nb-1.60Al	1023	0.150	$2.50 \times 10^{-29}$	
Ni-20Cr-6.3Nb-2.50Al	1023	0.220	$5.63 \times 10^{-29}$	
Ni-14.3Cr-4.4Al	1198	0.090	$1.01 \times 10^{-25}$	[32]
Ni-13.5Cr-5.8Al	1198	0.420	$1.70 \times 10^{-25}$	
Ni-9.3Co-11.79Al	973	0.160	$1.41 \times 10^{-29}$	[23]
Ni-9.5Co-12.60Al	973	0.240	$1.79 \times 10^{-29}$	
Ni-22.1Co-10.77Al	973	0.160	$1.09 \times 10^{-29}$	
Ni-21.7Co-13.40Al	973	0.310	$1.11 \times 10^{-29}$	

observed that the experimental values of  $k$  at higher volume fractions are greater than those predicted by the BWEM theory.

The variation of  $k$  predicted by the various theories at low volume fractions ( $< 20\%$ ) is very small. So in the lower range of volume fraction it is difficult to observe experimentally the variation of  $k$  with volume fraction. This problem seems to have arisen in the work of Seno *et al.* [7, 8] on the coarsening of cobalt precipitates in Cu-Co alloys, where they concluded that the  $k$  value is independent of volume fraction.

The volume fraction used ranged from 0.69% to 3.64%. According to the BWEM theory the  $k$  value should increase by about 35% over this range, which is rather small to be verified experimentally with confidence.

## 2.1. Coalescence

At high volume fractions the possibility of coalescence or encounters of two precipitates is very high. This phenomenon has been observed both in solid-phase systems [11, 25] and liquid-phase systems [5, 6]. Fig. 4

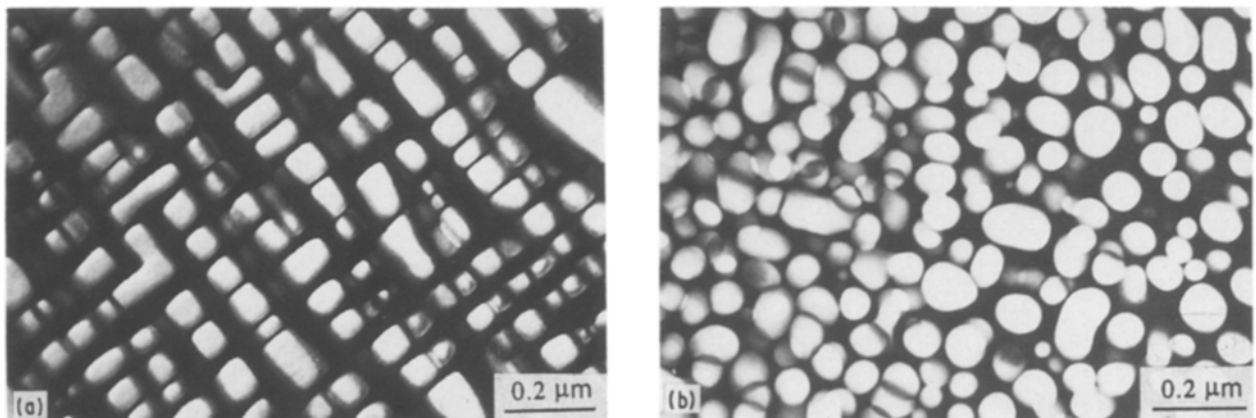


Figure 4 Dark-field micrographs showing coalesced particles in Ni-Al and Ni-Al-Cr alloys. (a) Ni-16.3 at % Al alloy aged at 973 K for 72 h. (b) Ni-9.7 at % Al-17.6 at % Cr alloy aged at 1023 K for 128 h.

TABLE II Comparison of  $k$  obtained by Kang and Yoon [5, 6] with that predicted by the BWEM theory

Alloy	Volume fraction	Exp. $k$ ratio	BWEM $k$ ratio
Cu-30Co	0.34	1.00	1.00
Cu-40Co	0.42	1.34	1.19
Cu-50Co	0.58	1.79	1.73
Cu-70Co	0.85	4.07	3.52
Cu-80Co	0.95	9.48	4.89
Cu-50Fe	0.59	1.00	1.00
Cu-70Fe	0.81	1.61	1.76
Cu-80Fe	0.90	3.00	2.20

shows microstructures of  $\gamma/\gamma'$  structures in Ni-Al and Ni-Al-Cr systems and some typical coalesced particles can be seen. There is some controversy over the physical mechanism of encounters. Davies *et al.* [11], based on their work in Ni-Co-Al alloys, proposed that if two precipitate particles grow close enough to each other they coalesce forming one particle. Essentially it involves overlapping of diffusion fields of the precipitate particles but not necessarily physical contact in the initial stage. Once the particles have coalesced, the resulting particle shape is then considered to change rapidly to the equilibrium shape by particle/matrix surface diffusion.

According to Doherty [34] coalescence occurs when the particles attract each other and move together. The driving force for this attraction is the removal of the elastically strained matrix between the two precipitates due to lattice parameters of the precipitate and matrix being different, i.e. the process depends on lattice mismatch. Doherty [34] substantiated his model of coalescence by referring to the results of Rastogi and Ardell [35] in which they found that as the lattice mismatch increased there was an increase in the maximum observed radius value and also the PSD broadened. However, in Al-Li alloys, although the lattice misfit was less than 0.1% the PSD was broad with an observed cut-off at 1.75 [36-38] and the statistical parameters of the PSDs were close to those predicted by the LSEM theory [11]. The LSEM theory models coalescence events independent of the exact mechanism by which it occurs, because the interaction volume for coalescence is a variable which may

simply be increased if there is a longer range interaction than assumed by Lifshitz and Slyozov [2] and Davies *et al.* [11]. Thus although the mechanism of coalescence is not established it is clear from particle morphologies that growth by a discontinuous mechanism does occur and should be incorporated in any coarsening model.

In Ni-Al alloys the ordered  $\gamma'$  (Ni<sub>3</sub>Al) phase is coherent with the matrix. When such particles are adjacent to each other there is a probability of 0.25 that they will be out of phase. If two such particles have to coalesce, an anti-phase boundary (APB) must be formed with an energy of 220 mJ m<sup>-2</sup> [39] which is very large compared to the destruction of two particle/matrix surfaces with an energy of about 10 mJ m<sup>-2</sup> [23]. This would result in an increase of energy if these particles coalesced and such an event is unlikely. This constraint on coalescence events has not been included in either the LSEM or BWEM theories but is easily accounted for by the inclusion of the probability value in the encounter integral, Equation 17.

A different mechanism of coalescence has been proposed in liquid-phase sintered systems. Kang and Yoon [6] proposed that when the grains touch each other the coalescence of grains takes place by a migration of the grain boundary between them towards the smaller grain. This may be due to rapid diffusion along the particle/matrix interface as soon as a neck is formed between two grains. Kang and Yoon [5] observed that the activation energy for coarsening remained constant with change in volume fraction, indicating that the dominant mechanism for coarsening of grains is still volume diffusion through the matrix even though the particles are touching each other.

### 3. Short-circuit diffusion of solute

For precipitates lying on high- or low-angle grain boundaries, the main solute diffusion paths are the grain boundaries themselves. Solute can also flow to the particle directly from the volume ( $D_v$ ) but this contribution to its growth is likely to be small except at very high temperatures.  $D_v$  may be so much smaller than  $D_{gb}$  that, though the diffusion cross-section is much larger for volume diffusion, the particle gets most solute from grain boundaries. Diffusion-controlled coarsening on low- and high-angle grain boundaries has been the subject of many studies [40-47]. The possible paths of solute to the growing precipitates other than due to volume diffusion are, (i) diffusion along the grain boundary, (ii) pipe diffusion along dislocations intersecting the precipitate surface, and (iii) diffusion along a dislocation line connecting two precipitates resulting in a direct mass transfer. Theories developed incorporating the above factors are along the lines of the LSW theory, i.e. the basic assumptions are the same.

When the coarsening process is limited by diffusion along the grain boundaries, the growth rate is given by [41-43, 46]

$$\frac{dr}{dt} = \frac{2\sigma V_m^2 C_e D_{gb} w}{3ABRT r^3} \left( \frac{r}{r_c} - 1 \right) \quad (18)$$

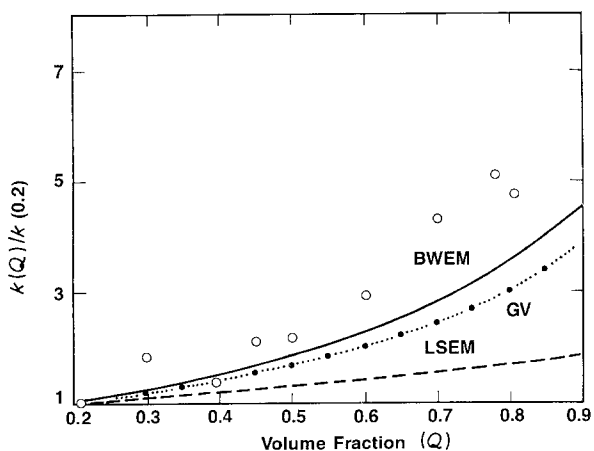


Figure 5 Comparison of  $k$  obtained by Courtney [79] ((O) Fe-Cu) with that predicted by the BWEM (—), LSEM (---) and GV (···) theories.

where  $D_{gb}$  is the diffusion coefficient for diffusion along the grain boundary,  $w$  is the grain-boundary thickness,  $A$  and  $B$  are constants and the rest of the terms have been defined previously. For coarsening by diffusion along dislocations the growth rate [47] is given by

$$\frac{dr}{dt} = \frac{ZqC_c\sigma V_m^2 D_d}{RT r^4} \left( \frac{r}{r_c} - 1 \right) \quad (19)$$

where  $Z$  is the number of dislocation lines crossing the surface,  $q$  is the dislocation pipe cross-section and  $D_d$  is the coefficient for diffusion along the dislocation. The size-distribution functions have been derived by Vengrenovitch [42, 45] for both cases. He discusses a transition from statistically uniform distribution to an ordered distribution at long ageing times. Physically one begins with the precipitates randomly distributed throughout the volume, a statistically uniform distribution. Those precipitates that lie on the dislocations or grain boundaries grow faster than the precipitates within the matrix. Thus, the precipitates not on dislocations or grain boundaries tend to be smaller in size, eventually falling below  $r_c$  and dissolving. This results in an ordered distribution of precipitates which lie only on grain boundaries and dislocations after very long ageing times.

The transition from a statistically uniform distribution to a preferentially ordered arrangement of particles on dislocations has been experimentally observed by Kreye [47] in an Ni–12.8 at % Al alloy aged at temperatures in the range 550 to 750°C. Also in work done on Al–Li alloys by Hosson [48] there is clear evidence of the faster growth of coherent precipitates lying on dislocations relative to the precipitates within the volume.

A dislocation has an associated strain field around it. Ardell and Nicholson [49] from their work on coarsening of  $\gamma'$  in Ni–Al alloys observed that the precipitates tend to grow only on one side of the dislocation while a precipitate-free zone was observed on the other side. From this they inferred [49] that the strain field of the dislocation results in favourable and unfavourable positions for growth of the precipitates. Studying the TEM photographs in [49] it is also evident that the precipitates lying on dislocations are, on average, larger than those in the matrix, further confirming that there is an effect of dislocations on coarsening.

Slyozov *et al.* [43] have discussed the coarsening kinetics for the situation where more than one mass transport mechanism operates simultaneously. They developed an expression for the effective diffusion coefficient which appears in the flux equation

$$\frac{dr}{dt} = \frac{D_{\text{eff}}}{r} (\bar{c} - c_r) \quad (20)$$

where  $D_{\text{eff}}$  is given by

$$D_{\text{eff}} = \frac{D(r)}{1 + D(r)/kr}$$

and

$$D(r) = D \left\{ 1 + \frac{a}{r} \left[ \frac{ND_{gb}}{2D \ln(2C/r)} \right] + \frac{MD_d^{1/2}}{[8D \ln(l/a)]^{1/2}} + \frac{D_d Z S_0}{Da4\pi\bar{r}(3Q_0/4\pi)^{1/3}} \right\}$$

where  $a$  is the lattice constant,  $M \approx 1$ ,  $l$  is the average length of the dislocation line,  $Z$  is the number of dislocation lines crossing the precipitate,  $S_0$  is the cross-section of the dislocation tube through which the mass transfer takes place,  $Q_0$  is the relative excess quantity of the material per unit volume and the rest of the terms have been defined previously. They conclude that when many mass transfer mechanisms are involved simultaneously, the cut-off value of  $\rho$ , i.e.  $r/\bar{r}$ , would be in the interval of 1 to 2. In contrast to the earlier mentioned modifications, Slyozov *et al.* [43] have accounted for various mass transfer effects by modifying the value of the effective diffusion coefficient appearing in the kinetic equation.

Clarendon and Fine [50] studied coarsening behaviour in Fe–Ni–Al–Mo alloys aged at 700°C. They compared their size distributions with other modified coarsening theories [11, 13, 21]. Though their kinetics obeyed  $\bar{r}^3 \propto t$ , the PSDs did not agree very well. They remarked that short-circuit diffusion paths may be responsible for the deviation of their results from the theories. Also, coarsening studies of  $\beta$ -precipitates in Al–11 wt % Mg alloy at 250°C [51] resulted in a higher value of interfacial energy and activation energy than expected. The reason for this anomalous result was suggested to be the occurrence of significant short-circuit diffusion at the ageing temperature.

Smith [52, 53] in a study of coarsening of manganese precipitates in magnesium and of  $UAl_2$  precipitates in uranium, observed cubic rate kinetics at high temperature. At lower temperatures, in  $\alpha$ -U, the exponent was between 4 and 5 suggesting that dislocation pipe diffusion controls the growth kinetics. This has also been verified by James and Fern [54].

To clarify the behaviour of precipitates coarsening on dislocations, specific studies of precipitation in cold-worked materials would be helpful.

#### 4. Elastic strains and elastic interactions

A precipitate present in a solid matrix has an excess energy associated with it. This energy can be split into three parts [55].

$$E = E_1 + E_2 + E_3 \quad (21)$$

$E_1$  is the elastic strain energy due to lattice mismatch between precipitate and matrix.  $E_2$  is the interfacial energy of the precipitate. The precipitate takes a particular shape so as to minimize  $E_1 + E_2$ . The third term,  $E_3$ , is the elastic interaction energy between precipitates due to overlap of the strain fields when the inter-particle distance becomes small. Owing to this elastic interaction non-spherical  $\gamma'$  precipitates in  $\gamma/\gamma'$  superalloys become aligned along  $\langle 100 \rangle$  directions. This effect has been used to produce rafted structures

in superalloys with improved high-temperature creep properties [56].

The nature of elastic interaction between two particles of equal shear modulus has been studied by several authors [49, 57–62] for different cases: (i) interaction between particles of equal shear modulus and of equal sizes embedded in an isotropic infinite matrix, (ii) interaction between particles of equal sizes embedded in an isotropic infinite matrix, and (iii) interaction between particles of equal shear modulus and dissimilar sizes embedded in an isotropic infinite matrix. As deduced by Eshelby [49, 57] the elastic interaction energy,  $E_3$ , between two precipitates A and B with equal shear moduli  $\mu'$  in a matrix with shear modulus  $\mu$  is

$$E_3 = \delta\mu \int_{V_A} (e_{ij}^B e_{ij}^B + 2e_{ij}^A e_{ij}^B) dV + \delta\mu \int_{V_B} (e_{ij}^A e_{ij}^A + 2e_{ij}^A e_{ij}^B) dV \quad (22)$$

where  $\delta\mu = \mu' - \mu$  and it is assumed that the transformation strain of each precipitate,  $e_{ij}$  is a pure dilation. Most coherent  $\gamma'$  precipitates satisfy this requirement, so this assumption simplifies the problem. Now

$$E_3 = E_d + E_s \quad (23)$$

where  $E_d$  is the direct interaction and  $E_s$  the shape-effect interaction.

$$E_d = \delta\mu \int_{V_A} (e_{ij}^B e_{ij}^B) dV + \delta\mu \int_{V_B} (e_{ij}^A e_{ij}^A) dV \quad (24)$$

$$E_s = 2\delta\mu \int_{V_A} (e_{ij}^A e_{ij}^B) dV + 2\delta\mu \int_{V_B} (e_{ij}^A e_{ij}^B) dV \quad (25)$$

From the expression for  $E_d$  it can be seen that  $E_d$  is less than zero if  $\delta\mu$  is less than zero, i.e. the particles will attract each other. If  $\delta\mu$  is more than zero the particles will repel. The sign of  $E_d$  is easy to inspect as the integrals are always positive. The same is not true for  $E_s$ . In the case of Ni<sub>3</sub>Al in nickel-solid solution it has been shown [49] that, though  $E_d$  is small in magnitude, it is sufficient to account for the alignment without the superimposed effect of  $E_s$ .  $E_d$  is large when particles are larger. There is no significant alignment at early stages of ageing, it becomes more pronounced as the size of the precipitates become larger and also it has been shown [49, 59, 60] that when the distance between particles,  $L$ , is large compared to the size of the particles themselves,  $E_3 \propto L^{-6}$ . For the case of homogeneous particles in an anisotropic matrix it has been shown [59, 61, 62] that  $E_3 \propto L^{-3}$  and also  $E_3$  is a function of orientation of the particles in the matrix.

The theoretical development due to Yamauchi and De Fontaine [58], based on microscopic theory of elasticity, has been applied by Miyazaki and co-workers [55, 63–66] in the study of the effect of elastic interactions on the morphology of  $\gamma'$  precipitates in nickel-base alloys. They observed that in certain alloys when the particles are very large, i.e. around 0.5  $\mu\text{m}$  and greater, the particles split into either two or eight particles.

Recently, Kachaturyan *et al.* [67] have developed a theoretical analysis to model morphological changes

occurring during coarsening of cubic-shaped precipitates. In the analysis they assumed that the elastic constants of both the precipitate and the matrix phases are approximately equal. The model predicts the following morphological shape transitions: (1) sphere  $\rightarrow$  cube,  $2a_0 \geq 7.7r_0$ , (2) cube  $\rightarrow$  doublet,  $2a_0 \geq 27r_0$ , (3) doublet  $\rightarrow$  octet,  $2a_0 \geq 82r_0$ , (4) octet  $\rightarrow$  platelet,  $2a_0 \geq 377r_0$ , where  $r_0$  is the ratio of the interfacial energy,  $\sigma$ , to the elastic energy per unit volume,  $E_1$ , and  $2a_0$  is the edge length of the cube. Knowing  $\sigma$  and  $E_1$  it is possible to predict the size at which these morphological changes occur. It can be easily seen that the predicted values of transitions strongly depend on the value of  $\sigma$  chosen to calculate them. Kachaturyan *et al.* [67] applied their analysis to  $\gamma'$  precipitates in the Ni–Al system and by taking a value of 12 mJ m<sup>-2</sup> for  $\sigma$ , predicted the morphological transitions at (1) sphere  $\rightarrow$  cube  $\approx$  7.7 nm, (2) cube  $\rightarrow$  doublet  $\approx$  30 nm, (3) doublet  $\rightarrow$  octet  $\approx$  90 nm, (4) octet  $\rightarrow$  plate  $\approx$  410 nm. Although there is a reasonable agreement between experiment and theory in the value of the transition from sphere to cube, the other transition values are found to be higher than the experimentally observed values [67]. This discrepancy is attributed to the finite perturbation required for a cube to split into a doublet or an octet or a platelet morphology thus allowing a cubic precipitate to retain its shape at larger sizes [67]. Also, by choosing a higher value of  $\sigma$ , the values of the predicted transitions will be higher. This model [67] implies that, as the particles grow beyond a certain size, they split into smaller particles due to the effects of elastic interaction, thus not permitting a continuous increase in the mean size with increase in ageing time. This leads to a possibility of stabilization of the microstructure. If this is true then one would expect discontinuities in the plot of mean size against time. Careful experimentation in a well-characterized system is needed to investigate this.

The splitting phenomenon is just the reverse of coalescence in the sense that splitting of precipitates leads to a discontinuous decrease in size. One of the arguments proposed for coalescence not taking place between two particles which are very close to each other but out of phase is the necessity of forming an APB. If two particles have instantaneously coalesced and the size corresponds to the size at which the particle should split according to the splitting model, then the question arises, will the particle coalesce in the first place? Morphology dependence on the size, arising out of the splitting model, may be an additional effect influencing the resistance to coalescence. A possible way of incorporating the splitting process in the coarsening theory is through the continuity equation. This will bring an additional term very similar to the encounter integral in the LSEM theory.

As we have discussed above, several investigations have been directed towards studying elastic interactions between two solid particles in a solid matrix. The effect this would have on the diffusion field during Ostwald ripening would be interesting but complex to study. Lifshitz and Slyozov [3] introduced the effect of elastic stress through the flux equation in the original



development of the LSW theory and they concluded that it does not effect the asymptotic nature of the particle-size distribution.

Ardell *et al.* [49] report that there is a resistance to coalescence due to the presence of elastic interactions. They also state that the kinetics of coarsening remain unaffected by their presence. When the lattice mismatch in alloy systems is small as in the case of the Ni–Al–Cr or Al–Li systems, where the precipitates are spherical in shape, there is no appreciable alignment. Although no systematic study has been made to observe the effect of lattice mismatch on particle coarsening, Ardell [30] has made a general observation that as the lattice mismatch increases, the greater is the particle size found at a particular ageing temperature. Although theoretical studies towards predicting the influence of elastic strains on the shape morphology of growing precipitates has been a topic of interest [55, 63, 66–68] its effect on the coarsening kinetics is yet to be resolved. Systematic experimental studies need to be done to study the effect of elastic strains on coarsening.

### 5. Loss of coherency

In most of the experimental work done on coarsening the precipitates were, and remained, coherent with the matrix. When the precipitate loses its coherency then the equilibrium solubility of the solute in the matrix decreases [69]. This would result in a change in the values of  $C_e$  and  $\sigma$  in the rate equation, but they change in opposite senses and counteract one another, although the change in  $\sigma$  would most likely be larger than the change in  $C_e$ .

### 6. Type of growth control

Recently [70–72], there has been some discussion on whether the particle growth-control mechanism is diffusion-, interface- or intermediate-type control.

White and Fisher [70] have studied precipitation and growth kinetics of  $\gamma'$  in Nimonic PE16 alloys based on resistivity experiments and have also re-interpreted data on  $\gamma'$  growth in Nimonic PE16 alloys [73]. In their theoretical development they define a term  $r^* = D/v$  where  $D$  is the diffusion coefficient of solute in the matrix and  $v$  is the “transfer velocity” of solute across the particle/matrix interface. The term  $r_c$  is the critical radius below which the growth is controlled by interface kinetics and above which it is controlled by volume-diffusion kinetics. They conclude [70] that most of the existing data on  $\gamma'$  coarsening falls in the transition region. The growth equation given by them is

$$f(\bar{r}) = At + \text{constant} \quad (26)$$

where  $f(\bar{r}) = (\bar{r}^2 + 8v\bar{r}^3/9D)$  and  $A = 64\sigma V_m C_e v / 81kT$ . White [71] has also developed expressions for the PSD evolved from the transition model. In the model the PSD is evaluated in terms of a parameter,  $\varepsilon$ , given by  $r^*/r_c$  where  $r^*$  is the critical radius for transition as described above, and  $r_c$  is the conventional critical radius. According to White [71], when  $\varepsilon < 1$  the PSD defined is for volume-diffusion-controlled growth with a cut-off at  $\rho = 1.5$  which is

the same as the LSW distribution and as  $\varepsilon$  increases the growth becomes interface controlled and the PSD broadens giving a higher cut-off value. In the theoretical development reported by White [71], with increase in ageing time the PSD approaches the LSW distribution.

Differentiating between a cubic or square dependence of the average particle size with time is difficult [72]. McLean has reviewed most of the experimental growth data on  $\gamma'$  in nickel-based alloys and by converting data obtained at different ageing temperatures to equivalent times at one temperature, has obtained data corresponding to ageing times of the order of years. McLean [72] concludes that the cubic rate law fits the experimental data better than the square rate law, confirming that coarsening in these systems is volume-diffusion controlled.

### 7. Particle motion

Both in the LSW theory and in the modified LSW theories the centre to centre distances of particles are assumed fixed, a reasonable assumption in solid precipitate–solid matrix systems. However, in liquid matrix–solid particle coarsening systems this assumption may not be reasonable. There are three sources of solid particle motion within a liquid: (i) Brownian motion; (ii) Stokes motion, i.e. particle settling (or rising) due to density differences between the liquid and solid; and (iii) convection currents.

Stevens [74] has calculated the velocity of a particle due to Brownian motion for solid matrix systems and concluded that rates of motion are insignificant compared with particle growth rates. However, the possibility of Brownian motion significantly affecting coarsening kinetics arises in liquid-matrix systems. Courtney [75–77] has analysed the effects of particle motion on coarsening in such systems. The time between particle contacts is exceptionally low for most liquid-phase sintered systems. Even a small density difference can lead to a large number of particle contacts per unit time. Assuming both Brownian motion and gravity as potential sources of contacts operating in parallel [78] the time between such contact is

$$\tau_b = \frac{\tau_g \tau_{br}}{\tau_g + \tau_{br}} \quad (27)$$

where  $\tau_g$  is the time between contacts due to gravity,  $\tau_{br}$  is the time between contacts due to Brownian motion. If Ostwald ripening contributes to coarsening in the system, then the equivalent time [77] for such a process to occur is given by

$$\tau_{rem} = \frac{\tau_r \tau_{or}}{\tau_r + \tau_{or}} \quad (28)$$

where  $\tau_r$  is the time required to fuse two particles,  $\tau_{or}$  is the time required to remove a particle from the system by Ostwald ripening. If  $\tau_b \gg \tau_{rem}$ , an isolated structure is formed.  $\tau_b$  varies rapidly with volume fraction;  $\tau_{rem}$  varies gradually with volume fraction. If  $\tau_b \ll \tau_{rem}$ , a contiguous skeleton-type structure is formed.  $\tau_r$  and  $\tau_{or}$  which affect  $\tau_{rem}$  depend on the volume fraction but not so strongly as  $\tau_b$ . The strong

dependence of  $\tau_b$  on volume fraction leads to an accelerated coarsening as the structure changes from isolated to the skeleton type of structure. In the isolated structure particles effectively are coarsened by Ostwald ripening but in skeleton structures coarsening is considered to occur by coalescence and Ostwald ripening [78].

Although in liquid-phase sintering coarsening of the solid-phase particles has been shown to follow the classical LSW volume diffusion kinetics [5, 6], the effects of particle motion on coarsening were not considered. The experimental data obtained by Courtney [79] have been compared with the predictions of the BWEM, LSEM and GV theories in Fig. 5. We see that the experimental data are consistently higher than the theoretical values indicating that the additional effects discussed in this section do, indeed, affect the coarsening kinetics.

A collision model of particle coarsening has been developed [80] which takes into account coalescence of particles from collisions caused by particle motion due to gravitational and fluid flow effects. This treatment could be incorporated in the coarsening theory through modification of the continuity equation.

Ratke and Thieringer [81] have developed a method to study the influence of particle motion on coarsening under three conditions, namely (i) all particles moving with a constant velocity relative to the matrix, (ii) particles driven by Marangoni-motion, and (iii) particles driven by Stokes motion. They brought in the effect of particle motion through the rate equation and neglected the effect of a finite volume fraction of particles. Their calculations are valid for both solid and liquid particles. Later Thieringer and Ratke [82] studied the coarsening behaviour of liquid lead particles moving at Stokes velocity in a liquid aluminium matrix and observed that the experimental PSD agreed well with their theoretical distribution. The volume fraction of lead particles was low, 0.04, due to removal of large particles from the liquid by sedimentation. This makes interpretation of the results in terms of coarsening rather difficult but is a consequence of earth-bound experiments.

Some experiments have been carried out in a space environment [83–85] to study the behaviour of alloy systems with a miscibility gap like the Zn–Pb system under microgravity conditions. Liquid-phase systems are chosen because the allowable time for the experiment is small. It has been shown by Kneissl *et al.* [86] that the necessary experimental conditions to study coarsening by Ostwald ripening of liquid lead droplets in near-monotectic Zn–Pb alloys without the effects of gravity segregation, can be obtained with proper design. Such experiments should assist in evaluating the effects of particle motion on coarsening kinetics.

## 8. Thermodynamically non-ideal systems

In the LSW theory the equation for the solute flux to the particle uses the Gibbs–Thomson equation which is based on ideal solution thermodynamics. Recently, Chaix *et al.* [87, 88] modified the LSW theory to

account for significant solid solubility of the main constituent of the matrix phase in the particles and also departure from ideality of the matrix solution phase. The modified LSW rate equation is given by

$$\bar{r}^3 - \bar{r}_0^3 = \frac{U_A}{(1 - X_B^{\text{os}})} k_{\text{LSW}}(t - t_0) \quad (29)$$

where  $U_A$  is the driving force correction factor, which does not depend on the particle radius. The influence of the departure from ideal solution and the effect of solid solubility [87] appears in the above equation through the factor  $U_A/(1 - X_B^{\text{os}})$ . They compared their theoretical predictions with experimental data on W–Ni–Cr liquid-phase sintered materials and explained the experimentally observed growth-rate dependence on composition. Deviation from ideality will also affect the value of the diffusion coefficient of the solute and should also be considered. Recently, liquid-phase sintering experiments in the Fe–Cu and Co–Cu systems have shown that inclusion of the thermodynamic factor is necessary in order for coarsening theories to predict accurately experimental growth rates [89]. This factor will also be important in solid-state systems, for example, in the Ni–Al system the thermodynamic factor modifies the growth rate constant by  $\approx 0.24$ , resulting in a larger value for the particle matrix surface energy determined from experimental rate constant data [89].

## 9. Multi-phase precipitates

Slyozov and Sagalovich [90] have studied the problem of coarsening of multi-phase precipitates. The basic approach is similar to that adopted by Lifshitz and Slyozov [2]. For a system with  $N$  components and having  $k$  phases the diffusion flux equation is given by

$$J_{ir}^s = \frac{D_i n_0}{r} (\bar{c}_i - c_{ir}^e) \quad (30)$$

where  $J_{ir}^s$  is the flux of the  $i$ th component for the  $s$ th phase,  $D_i$  is the diffusion coefficient of the  $i$ th component,  $n_0$  is the number of atoms per unit volume,  $\bar{c}_i$  is the average concentration of the  $i$ th component in the matrix and  $c_{ir}^e$  is the equilibrium concentration of the  $i$ th component at the  $s$ th phase particle/matrix interface. For each of the  $k$  phases there is a continuity equation similar to Equation 8. Similarly there is a kinetic equation for each phase analogous to Equation 3. Slyozov and Sagalovich [90] deduce that the growth of the individual phases in a multi-component system still corresponds to  $\bar{r}^3 \propto t$  kinetics. No systematic studies of the coarsening of multi-phase particles have been reported in the literature. A possible model system for such a study would be the Ni–Al–Cr system where both chromium and  $\gamma'$  particles coarsen together in a nickel matrix.

## 10. Conclusions

The classical LSW theory has been applied to the coarsening process in many different kinds of systems with excellent qualitative agreement. LSW theory has been modified by several people to account for the volume fraction of second-phase particles and these modified theories predict dependence of the rate

constant,  $k$ , on the volume fraction of second-phase particles. Published experimental coarsening data have been either over a narrow range of volume fraction or from the experiments carried out on multi-component systems. This has made it difficult to evaluate critically the various coarsening theories based on those experimental data. Coarsening experiments conducted with the objective of testing the theories should be designed to permit control of the numerous parameters involved. This may be achieved by carrying out experiments with solid and liquid matrices and under microgravity conditions. More extensive evaluation of coarsening data are required, beyond the time dependence of the growth rate and the form of the particle-size distribution. For example, growth-path envelope analysis may be applied [91] to experimental data to determine growth rates as a function of time and critical radii,  $r_c$ .

It is clear from the preceding discussion that an opportunity exists to modify the coarsening theory to take into account various factors expected to affect the coarsening kinetics to some extent. The solid foundation of the LSW theory may be built upon to generalize coarsening theory to take account of these factors. Not all of the factors discussed above operate in every system and in some cases the effect may be negligible. However, the attempt to refine the current theory is worthwhile because it may then be applied with more confidence to predict coarsening behaviour in the many systems in which it occurs. It may also be used to determine important quantities such as particle/matrix surface energies which are often difficult to determine by other methods.

Modifications to the LSW theory can be made through the kinetic equation (Equation 3) or through the continuity equation (Equation 8), depending upon the effect being taken into account. Such modifications have been made for most of the factors thought to affect coarsening and so the theoretical treatments are readily available. It remains for these individual modifications to be combined to generalize the theory. Introduction of other effects into the coarsening theory will refine it further and we believe will lead to improved agreement with experiment.

## Acknowledgements

We thank Dr R. N. Stevens, Queen Mary College, University of London, UK, for the provision of a computer programme and analysis incorporating the self-consistent treatment of the BW theory with the LSEM theory. This work was supported by NSF under grant no. DMR-8043983, and is based on material submitted by C. S. Jayanth in partial fulfilment of the requirement for the PhD degree, Illinois Institute of Technology.

## References

1. G. W. GREENWOOD, *Acta Metall.* **4** (1956) 243.
2. I. M. LIFSHITZ and V. V. SLYOZOV, *Phys. Chem. Solids* **11** (1961) 35.
3. *Idem*, *Fizika. Ivergoda. Tela*, **1** (1959) 1401.
4. C. WAGNER, *Z. Electrochem.* **65** (1961) 581.
5. S. S. KANG and D. N. YOON, *Met. Trans.* **13A** (1982) 1405.
6. *Idem, ibid.* **12A** (1981) 65.
7. Y. SENO, Y. TOMOKIYO, K. OKI and T. EGUCHI, *Trans. Jpn Inst. Metals* **24** (1983) 491.
8. T. EGUCHI, Y. TOMOKIYO, K. OKI and Y. SENO, *Mat. Res. Soc. Symp. Proc.* **21** (1984) 475.
9. R. WATANABE and Y. MASUDA, *Modern Devel. Powder Metall.* **6** (1974) 1.
10. R. WATANABE, K. TADA and Y. MASUDA, *Z. Metallkde* **13** (1976) 619.
11. C. K. L. DAVIES, P. NASH and R. N. STEVENS, *Acta Metall.* **28** (1980) 179.
12. A. J. ARDELL, *Acta Metall.* **20** (1972) 61.
13. K. TSUMURAYA and Y. MIYATA, *ibid.* **31** (1983) 437.
14. R. N. STEVENS, personal communication (1978).
15. P. NASH, *Scripta Metall.* **18** (1984) 295.
16. R. ASIMOV, *Acta Metall.* **11** (1963) 71.
17. A. D. BRAILSFORD and P. WYNBLATT, *Acta Metall.* **27** (1979) 489.
18. P. W. VOORHEES and M. E. GLICKSMANN, *ibid.* **32** (1984) 2001.
19. *Idem, ibid.* **32** (1984) 2013.
20. J. A. MARQUSEE and J. ROSS, *J. Chem. Phys.* **80** (1984) 536.
21. M. TOKUYAMA and M. KAWASAKI, *Physica* **123A** (1984) 386.
22. P. W. VOORHEES, *J. Stat. Phys.* **38** (1985) 231.
23. C. K. L. DAVIES, P. NASH and R. N. STEVENS, *J. Mater. Sci.* **15** (1980) 1521.
24. A. J. ARDELL and R. B. NICHOLSON, *J. Phys. Chem. Solids* **27** (1966) 1793.
25. D. J. CHELLMAN and A. J. ARDELL, *Acta Metall.* **22** (1974) 577.
26. D. W. CHUNG and M. CHATURVEDI, *Metallogr.* **8** (1975) 329.
27. P. NASH, PhD thesis, The University of London, Queen Mary College, London (1977).
28. M. CHATURVEDI and D. W. CHUNG, *J. Inst. Metals* **101** (1973) 253.
29. H. GLEITER and E. HORNBOGEN, *Z. Metallkde* **58** (1967) 157.
30. A. J. ARDELL, *Met. Trans.* **1** (1970) 525.
31. T. B. GIBBONS and B. E. HOPKINS, *Met. Sci. J.* **5** (1971) 233.
32. V. BISS and D. L. SPONSELLER, *Met. Trans.* **58** (1973) 1953.
33. YU. G. SOROKINA and S. A. YUGANOVA, *Metall. Term. Obra. Metallov.* **6** (1968) 46.
34. R. D. DOHERTY, *Metal Sci.* **16** (1982) 1.
35. P. K. RASTOGI and A. J. ARDELL, *Acta Metall.* **19** (1971) 321.
36. B. P. GU, G. L. LIEDL, J. H. KULWICKI and T. H. SANDERS Jr, *Mater. Sci. Engng* **70** (1985) 217.
37. B. P. GU, G. L. LIEDL, K. MAHALINGAM and T. H. SANDERS Jr, *ibid.* **78** (1986) 71.
38. K. MAHALINGAM, B. P. GU, G. L. LIEDL and T. H. SANDERS Jr, *Acta Metall.* **35** (1987) 483.
39. F. A. FLINN, *Trans. AIME* **218** (1960) 145.
40. A. J. ARDELL, *Acta Metall.* **20** (1971) 601.
41. H. O. K. KIRCHNER, *Met. Trans.* **2** (1971) 2861.
42. R. D. VENGRENOVITCH, *Acta Metall.* **30** (1982) 1079.
43. V. V. SLYOZOV, V. V. SAGALOVICH and L. V. TANATROV, *J. Phys. Chem. Solids* **39** (1978) 705.
44. M. V. SPEIGHT, *Acta Metall.* **16** (1968) 133.
45. R. D. VENGRENOVITCH, *Fiz. Metal. Metalloved.* **39** (1975) 436.
46. G. W. GREENWOOD, "The Mechanism of Phase Transformation in Crystalline Solids", Manchester, Institute of Metals Monograph, No. 33 (1968).
47. H. KREYE, *Z. Metallkde* **61** (1970) 108.
48. J. D. HOSSON, *Beitr. Elektro. Direktabb. Oberfl.* **16** (1983) 169.
49. A. J. ARDELL, R. B. NICHOLSON and J. D. ESH-ELBY, *Acta Metall.* **14** (1966) 1295.
50. H. CLARENDON and M. E. FINE, *Mater. Sci. Engng* **63** (1984) 197.

51. S. I. KWUN and M. E. FINE, *Met. Trans.* **16A** (1985) 709.
52. A. F. SMITH, *Acta Metall.* **15** (1967) 1867.
53. *Idem*, *J. Less-Common Metals* **9** (1965) 233.
54. P. F. JAMES and F. H. FERN, *J. Nucl. Mater.* **29** (1969) 203.
55. T. MIYAZAKI, H. IMAMURA and T. KOZAKI, *Mater. Sci. Engng* **54** (1982) 9.
56. R. A. MacKAY and L. J. EBERT, *Met. Trans.* **16A** (1985) 1969.
57. J. D. ESHELBY, *Proc. Roy. Soc.* **A241** (1957) 376.
58. H. YAMAUCHI and D. de FONTAINE, *Acta Metall.* **27** (1979) 763.
59. W. C. JOHNSON and J. K. LEE, *Met. Trans.* **10A** (1979) 1141.
60. E. H. YOFFE, *Phil. Mag.* **30** (1974) 923.
61. A. G. KHACHATURYAN, *Sov. Phys. Sol. State* **8** (1967) 2163.
62. E. SEITZ and D. de FONTAINE, *Acta Metall.* **26** (1978) 1671.
63. T. MIYAZAKI, H. IMAMURA, H. MORI and T. KOZAKI, *J. Mater. Sci.* **16** (1981) 1197.
64. M. DOI, T. MIYAZAKI and T. WAKATSUKI, *Mater. Sci. Engng* **67** (1984) 247.
65. *Idem*, *ibid.* **74** (1985) 139.
66. M. DOI and T. WAKATSUKI, *ibid.* **78** (1986) 87.
67. A. G. KHACHATURYAN, S. V. SEMENOVSKAYA and J. W. MORRIS Jr, *Acta Metall.* (1986).
68. P. W. VOORHEES, abstract 116th TMS Annual Meeting, Denver, Colorado, 23–26 February (1987).
69. P. K. RASTOGI and A. J. ARDELL, *Acta Metall.* **17** (1969) 595.
70. R. J. WHITE and S. B. FISHER, *Mater. Sci. Engng* **33** (1978) 149.
71. R. J. WHITE, *ibid.* **40** (1979) 15.
72. D. McLEAN, *Met. Sci.* **18** (1984) 249.
73. J. I. BRAMMAN, A. S. FRASER and W. H. MARTIN, *J. Nucl. Energy* **25** (1971) 223.
74. R. N. STEVENS, personal communication (1981).
75. T. H. COURTNEY, *Met. Trans.* **8A** (1977) 671.
76. *Idem*, *ibid.* **8A** (1977) 679.
77. *Idem*, *ibid.* **8A** (1977) 685.
78. A. N. NIEMI, L. E. BAXA, J. K. LEE and T. H. COURTNEY, *Modern Devel. Powder Metall.* **12** (1980) 483.
79. P. W. VOORHEES and M. E. GLICKSMAN, *Met. Trans.* **15A** (1984) 1081.
80. U. LINDBORG and K. TORESELL, *Trans. AIME* **242** (1986) 94.
81. L. RATKE and W. K. THEIRINGER, *Acta Metall.* **33** (1985) 1793.
82. W. K. THEIRINGER and L. RATKE, *ibid.* **35** (1987) 1237.
83. C. Y. ANG and L. L. LACY ASTP Experiment MA-044, NASA TM X-64956, Marshall Space Flight Center, Alabama (1975).
84. H. AHLBORN and K. LEOHBERG, Proceedings Status Seminar Uber Spacelab-Nutzung, Bad Kissingen, European Space Agency, Hamburg FRG 12 (1976).
85. T. CARLBERG and H. FREDRICKSSON, Proceedings of the 3rd European Symposium on Material Sciences in Space, edited by T. D. Guyenne and S. Adany, European Space Agency, Paris. Grenoble (1979) p. 233.
86. A. KNEISSL, P. PFFEFFERKON and H. FISCHMEISTER, Proceedings of the 4th European Symposium on Material Sciences under Microgravity, Madrid (1983) p. 55.
87. J. M. CHAIX, N. EUSTATHOPOULOS and C. H. ALLIBERT, *Acta Metall.* **34** (1986) 1589.
88. *Idem*, *ibid.* **34** (1986) 1593.
89. S. C. YANG and P. NASH, *J. Mater. Sci. Tech.* **4** (1988) 860.
90. V. V. SLYOZOV and V. V. SAGALOVICH, *J. Phys. Chem. Solids* **38** (1977) 943.
91. C. S. JAYANTH, PhD thesis, Illinois Institute of Technology, Chicago, Illinois, USA (1988).

*Received 5 May  
and accepted 4 September 1988*